

Collisionless dynamo seeds from phase mixing-induced electron slippage

István Pusztai* and Lise Hanebring

Department of Physics and Astronomy, Chalmers University of Technology, Gothenburg 41296, Sweden

James Juno

Princeton Plasma Physics Laboratory, Princeton, New Jersey 08543, USA

(Dated: June 29, 2026)

Magnetic fields permeating the Universe on the largest astrophysical scales are thought to result from dynamo amplification in weakly collisional turbulence, but the origin of the seed fields remains an open problem of cosmic magnetogenesis. We identify a kinetic mechanism for magnetic-field generation in initially unmagnetized, collisionless plasmas, arising from phase-mixing-induced braking of spatially varying electron flows. Using analytical theory, fully kinetic Vlasov simulations, and turbulent scaling arguments, we show that this process generates coherent magnetic seed fields on scales far larger than the characteristic kinetic scales of the plasma, with strengths comparable to or exceeding classical Biermann battery estimates. The mechanism requires neither a finite initial magnetic field nor misaligned thermodynamic gradients and occurs naturally in electron-ion plasmas.

Magnetic fields permeate the Universe on all scales up to the largest gravitationally bound structures [1–6], regulating momentum and heat transport [7–11] and cosmic-ray propagation, and playing an important role in particle acceleration [12–15] as well as the formation of galaxies and stars [16, 17]. Understanding the origin of cosmic magnetization therefore remains a fundamental problem.

Observations indicate magnetic field energy densities in galaxies and clusters in near equipartition with the kinetic energy in their turbulent flows. Thus these fields are believed to result from turbulent dynamo amplification operating in weakly collisional astrophysical plasmas [18–20]. Dynamo action, however, requires a pre-existing seed field [5, 21, 22], the origin of which remains debated. Proposed mechanisms include primordial magnetogenesis in the early Universe, magnetic fields generated during cosmological phase transitions, the Biermann battery [23] operating in ionization fronts. However, the resulting field amplitudes are typically weak [3, 24, 25], motivating the search for additional sources of coherent seed fields.

The Weibel instability [26] provides an alternative route to magnetic-field generation [27–30], efficiently converting free energy associated with pressure anisotropy into magnetic fields and rapidly magnetizing initially unmagnetized plasmas [31]. However, the resulting fields are generated on kinetic scales, and their relevance for large-scale magnetogenesis depends on the efficiency of subsequent transfer of magnetic energy to larger scales [32]. While recent kinetic studies have demonstrated substantial scale growth of Weibel-generated fields, the extent to which such fields can provide large-scale dynamo seeds remains an active area of investigation.

At the same time, numerical studies of collisionless astrophysical dynamos have undergone rapid development [28, 33–36], revealing rich multiscale processes absent

from conventional magnetohydrodynamic modeling [37–43] and potentially contributing to magnetic-field generation. Most such studies have employed hybrid-kinetic models or electron-positron plasmas, while fully kinetic simulations of electron-ion plasmas are only now becoming computationally accessible.

In this Letter we identify a kinetic mechanism for magnetic-field generation in initially unmagnetized electron-ion plasmas. The mechanism relies on phase mixing of spatially varying electron flows. Although electrons and ions are initially current-neutral, phase mixing reduces the electron flow while the ion flow remains nearly unchanged, producing a current that self-consistently generates magnetic fields. Using analytical theory, fully kinetic Vlasov simulations, and turbulent scaling arguments, we show that the resulting fields constitute a competitive source of large-scale magnetic seeds and may play a role both in cosmic magnetogenesis and in the dynamics of collisionless electron-ion plasmas.

We consider the generation of magnetic fields in a collisionless, non-magnetized electron-proton plasma, from an initial bulk flow of the form $V_y(x, 0) = V_0 \exp(ikx)$, identical for both species. The characteristic timescale of the process is the electron phase mixing time $t_{\text{pm}} = (kv_{te})^{-1}$ – with $v_{te} = \sqrt{2T_e/m_e}$, T_e and m_e denoting the thermal speed, the temperature and the mass of electrons – which allows us to disregard the much slower ion dynamics. Furthermore, we expand the near-Maxwellian electron distribution $f_e(\mathbf{x}, \mathbf{v}, t)$ in $V_0/v_{te} \ll 1$ for the assumed subsonic flow velocities as $f_e \approx f_0 + f_1$, where $f_0 = n/(\sqrt{\pi}v_{te})^3 \exp[-(v/v_{te})^2]$, n is the electron density and $f_1(t=0) = (2V_0v_y/v_{te}^2) \exp(ikx)f_0$.

To find the evolution of the electron current we start from the kinetic equation, where we neglect acceleration by the magnetic field. With the notation $X = \hat{X} \exp(ikx)$, and e for the elementary charge, it reads

$$\partial_t \hat{f}_1 + ikv_x \hat{f}_1 = \frac{e}{m_e} \hat{E}_y(t) \frac{\partial f_0}{\partial v_y}. \quad (1)$$

* pusztai@chalmers.se

Then, similar to a Landau damping calculation we solve the initial value problem using the one-sided Laplace transform $\tilde{X}(\omega) = \int_0^\infty dt \exp(i\omega t) \hat{X}(t)$. This allows us to obtain an algebraic equation, from which \tilde{f}_1 can be expressed as

$$\tilde{f}_1 = i \frac{2V_0 v_y f_0 / v_{te}^2}{\omega - kv_x} + i \frac{e}{m_e} \frac{\partial v_y f_0}{\omega - kv_x} \tilde{E}_y(\omega). \quad (2)$$

The current that develops originates from the phase-mixing-induced slippage between the electron and ion flows thus $j_y(t) = enV_0 - e \int v_y f_1 d^3v$. The Laplace transform and the velocity integrals can be carried out in terms of the plasma dispersion function $Z(\zeta) = \pi^{-1/2} \int_{-\infty}^\infty dt e^{-t^2} / (t - \zeta)$, to find

$$\tilde{j}_y(\omega) = i \frac{enV_0}{\omega} [1 + \zeta Z(\zeta)] + \frac{i\epsilon_0 \omega_{pe}^2}{kv_{te}} Z(\zeta) \tilde{E}_y(\omega), \quad (3)$$

where $\zeta = \omega / (kv_{te})$, and $\omega_{pe} = \sqrt{ne^2 / (\epsilon_0 m_e)}$ is the electron plasma frequency with ϵ_0 the vacuum permittivity.

The process operates on time scales, where the displacement current can be neglected, thus Ampère's and Faraday's laws imply $\tilde{E}_y = (i\omega\mu_0/k^2)\tilde{j}_y$, which allows us to eliminate \tilde{E}_y from (3), and solve for \tilde{j}_y . Finally, introducing the electron inertial length $\delta_e = c/\omega_{pe}$, we inverse transform back to obtain an expression for time-dependent current amplitude

$$\hat{j}_y(t) = \frac{enV_0}{2\pi} \int_{-\infty}^\infty d\omega e^{-i\omega t} \frac{i}{\omega} \frac{1 + \zeta Z(\zeta)}{1 - \frac{1}{k^2 \delta_e^2} \zeta Z(\zeta)}. \quad (4)$$

While ready to numerical evaluation, this integral cannot be expressed in a closed form. It is however interesting to consider its short and long time limits. The $|\omega| \rightarrow \infty$ limit corresponds to the early time behavior. Using the appropriate expansion $Z(\zeta) \approx -\frac{1}{\zeta} - \frac{1}{2\zeta^3} - \dots$ leads to

$$\hat{j}_y(t) \approx enV_0 \frac{k^2 v_{te}^2}{4} \left(1 + \frac{1}{k^2 \delta_e^2}\right)^{-1} t^2. \quad (5)$$

Note that this expression is similar to the early-time limit of the pure free streaming result – which can be found exactly using the method of characteristics – except that it is reduced by the factor $[1 + 1/(k^2 \delta_e^2)]^{-1} \approx k^2 \delta_e^2 \ll 1$ due to the inductive response of the system.

The long time asymptotic behavior is given by $|\omega| \rightarrow 0$ limit, when $Z(\zeta) \approx i\sqrt{\pi} - 2\zeta + \dots$. If we in addition assume the astrophysically relevant limit of $k^2 \delta_e^2 \ll 1$, we find the approximate solution

$$\hat{j}_y(t) \approx enV_0 [1 - e^{-\gamma t}]. \quad (6)$$

Thus, the system evolves towards the state where all electron flow is phase-mixed away, and the remaining ion flow represents a current of amplitude enV_0 . The rate of approaching this state is given by the zero of the denominator of the integrand, which in the appropriate limit

yields $1 - i\sqrt{\pi} \frac{1}{k^2 \delta_e^2} \zeta = 0$. It is solved by a purely imaginary frequency corresponding to $\gamma = k^3 \delta_e^2 v_{te} / \sqrt{\pi}$; this coincides with the known damping rate [35, 44] of magnetic perturbations of non-magnetized collisionless plasmas, where the current is carried by electron flows. Here the current arises due to a slippage of electrons compared to the ion flow.

Our simplification of neglecting the impact of the magnetic field breaks down well before Eq. (6) would approach its asymptotic value, corresponding to $B_{\text{asy}} \sim \mu_0 enV_0 / k$. An upper bound for the magnetic field saturation level is given by requiring the field to marginally magnetize thermal electrons at the scale k^{-1} , yielding $B_{k\rho_e \sim 1} \sim kv_{te} m_e / e$. A lower bound is given by assuming that saturation happens on the phase mixing time scale, which is the shortest relevant timescale in the process. Inserting $t \sim t_{\text{pm}}$ into the $k^2 \delta_e^2 \ll 1$ limit of (5) yields

$$B_{t \sim t_{\text{pm}}} \sim \frac{kV_0 m_e}{e} = B_{\text{asy}} k^2 \delta_e^2. \quad (7)$$

We note that, since $B_{k\rho_e \sim 1} / B_{t \sim t_{\text{pm}}} = v_{te} / V$, on the timescale that would be required for reaching $B_{k\rho_e \sim 1}$ ion phase mixing also becomes non-negligible, for comparable species temperatures and nearly sonic flow speeds. The analytical theory provides the early-time evolution of the slippage field together with physically motivated bounds on its saturation amplitude. Establishing the nonlinear evolution between these bounds, and determining the resulting saturation level, however, requires a first-principles kinetic simulations.

In the following, we employ the Vlasov–Maxwell solver [45] of the continuum plasma simulation framework GKEYLL [46] to demonstrate that saturation occurs between the bounds $B_{t \sim t_{\text{pm}}}$ and $B_{k\rho_e \sim 1}$, and to verify the expected linear scaling with k in the regime $k\delta_e \ll 1$. We perform Vlasov simulations of an electron–proton plasma with the physical mass ratio $m_i/m_e \approx 1836$, using one spatial and two velocity dimensions. Both species are initialized with spatially homogeneous Maxwellian distributions at equal, nonrelativistic temperatures, $T_i^{(t=0)} = T_e^{(t=0)}$, corresponding to $v_{te}/c = 0.0626$, and share an initial sinusoidal flow $V_y = V_0 \sin(kx)$. The simulation domain is periodic, with size L chosen to accommodate a single wavelength of the perturbation, $k_0 = 2\pi/L$. Apart from using a non-relativistic formulation of the Vlasov equation for these simulations, the solver does not rely on further approximations.

In our baseline case, the flow is mildly subsonic, $V_0 = 0.35 c_s$, where the sound speed is $c_s = \sqrt{T_e/m_i}$, with the ion mass m_i . The largest simulation domain considered is $L = 277.7 \delta_e$, corresponding to $t_{\text{pm}} \omega_{pe} = 706.4$. We employ a spatial resolution of $\Delta x = 0.27 \delta_e$, discretize the ± 3 species thermal speed wide velocity domain using 32 uniformly spaced cells, and represent the distribution functions within each phase space cell using second-order polynomial basis functions.

As seen in Fig. 1, the kinetic simulation result (black solid) closely follows the analytical result (blue dashed) – given by Eq. (4) – until around $t = 19t_{\text{pm}}$, at which point the kinetic simulation exhibits saturation and levels off. Since $k\delta_e \ll 1$, the closed form approximate result, Eq. (6) (gray dotted), is a good estimate of the evolution of the analytical result, except at very early times when the increase is $\propto t^2$.

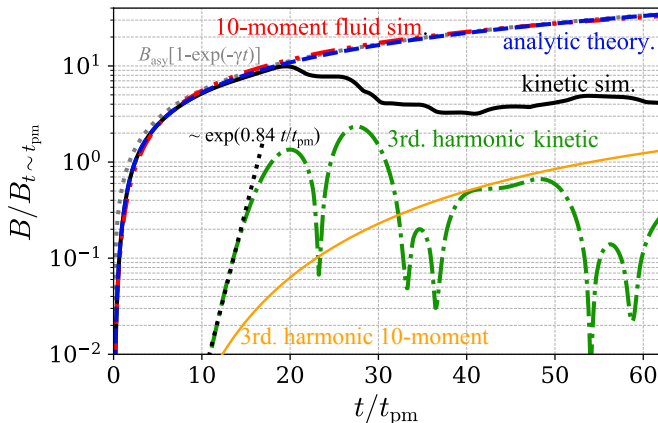


FIG. 1. Time evolution of magnetic field amplitude, normalized to $B_{t \sim t_{\text{pm}}}$. Solid black: kinetic simulation; blue dashed: linear theory, corresponding to Eq. (4); gray dotted: theory long time asymptote, corresponding to Eq. (6); red dash-dot-dot: 10-moment fluid simulation; green dash-dotted: 3rd harmonic in kinetic simulation; thin solid orange: 3rd harmonic in 10-moment simulation; black dotted line shows $\propto \exp(0.84 t/t_{\text{pm}})$ for reference.

Preceding the saturation in the kinetic simulation, the odd harmonics of k_0 grow exponentially with growth rates $\sim 1/t_{\text{pm}}$. This is illustrated by showing the 3rd harmonic (green dash-dotted) and its fitted exponential growth (black dotted) in Fig. 1. The harmonics stop growing at the same time the saturation occurs and their total root-mean-square amplitude remains almost an order of magnitude lower than that of the main mode. Although phase mixing generates the pressure anisotropy required to drive the Weibel instability, the electron-Weibel growth rate at the long wavelengths considered here (e.g., the third harmonic) is orders of magnitude too small to explain the observed exponential growth. In addition, the observed lack of growth of the even harmonics is another strong indication that the observed growth is not caused by Weibel instability.

That the growth of harmonics occurs at a wide range of wavenumbers is illustrated in Fig. 2, where the time evolution of only the odd harmonics of k_0 are shown until the time of saturation. All plotted wavenumbers, besides k_0 , grow exponentially on t_{pm} timescales with comparable growth rates. We note that in additional simulations (not shown here) that host Weibel instability with sizable growth rates, significant linear-phase Weibel growth is localized in the vicinity of the most unstable mode, and it is clearly distinguished from the odd harmonics of

the phase-mixing slippage field appearing at long wavelengths. However the nonlinear saturation of the Weibel instability also involves the development of odd harmonics, these spectral features inherit the breadth of the peak appearing in the linear growth phase.

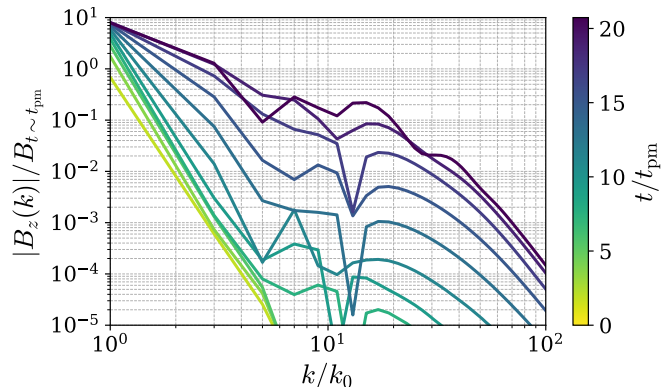


FIG. 2. Time evolution of the magnetic field spectrum. Only those wavenumbers that are odd multiples of $k_0 = 2\pi/L$ are plotted, as even harmonics remain negligible.

It is illuminating to model the same scenario using the 10-moment fluid solver [47, 48] of GKEYLL, which evolves the collisionless hierarchy of fluid equations up to the full pressure tensor for each species α . Here we use a pressure isotropization heat flux closure [47] $\partial_k q_{ij,k,\alpha} = k_{0\alpha} v_{\text{th},\alpha} (p_{ij,\alpha} - p_\alpha \delta_{ij})$ where $q_{ijk,\alpha}$ and $p_{ij,\alpha}$ are elements of the the heat flux and the pressure tensors, p_α is the scalar pressure, and $k_{0\alpha}$ is a parameter that sets the isotropization strength. At sufficiently high mass ratio k_{0i} sets the damping rate of the mass flow, while k_{0e} affects the damping rate of the magnetic field when the current is carried by electrons, as described in Ref. [36]. The ten-moment model captures sufficient information about the phase-space structure that, similarly to magnetic field damping, it can approximately reproduce the dynamics of the stress developing due to phase-mixing breaking the electron flow, and the rate of the corresponding electron slippage is effectively tuned by k_{0e} . When using $k_{0i}/k_0 = 100$ to reduce ion flow damping to negligible values, $k_{0e}/k_0 = 1.1$ yields a close agreement between the magnetic field growth predicted by Eq. (4) and the 10-moment simulation; compare the blue dashed and red dash-dot-dot curves in Fig. 1. Importantly, the fluid result does not saturate during the simulation time and, unlike the kinetic simulation, the growth of odd harmonics is polynomial instead of exponential (see thin orange line in Fig. 1). This suggests that the saturation observed in the kinetic simulation has an origin involving finer structures in the distribution function.

To determine the wavenumber scaling of the saturation field strength, we perform a scan in $k\delta_e$, extending down to $k\delta_i \sim 1$, as shown in Fig. 3. Here B_{sat} is normalized to $B_{t \sim t_{\text{pm}}}$, and the simulations use $V_0 = 0.0035 c_s$. The ratio $B_{\text{sat}}/B_{t \sim t_{\text{pm}}}$ approaches a finite asymptotic value as

$k\delta_e \rightarrow 0$, implying $B_{\text{sat}} \propto k$ in the long-wavelength limit. Additional parameter scans further establish empirically that

$$B_{\text{sat}} \sim (v_{te}/V_0)^{1/3} k V_0 m_e / e. \quad (8)$$

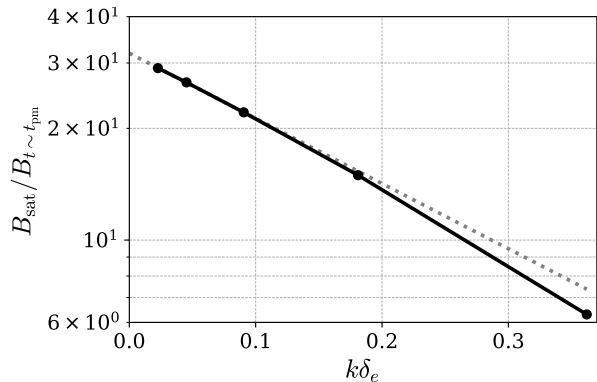


FIG. 3. Convergence of $B_{\text{sat}}/B_{t \sim t_{\text{pm}}}$ at low $k\delta_e$ values. Black markers correspond to simulations. Gray dotted line shows $\propto \exp(-4.05 k\delta_e)$ for reference.

The saturation observed in the kinetic simulations is closely related to the growth of odd harmonics of the magnetic field, suggesting a nonlinear harmonic-transfer process as a possible saturation mechanism. The Lorentz force associated with the fundamental current and magnetic field contains a component at twice the fundamental wavenumber. This force distorts the current profile and generates a third-harmonic component, leading to a hierarchy of odd magnetic harmonics, while even harmonics remain weak due to the parity of the nonlinear coupling.

To estimate the resulting saturation amplitude, let $\Omega_e = eB/m_e$ denote the electron cyclotron frequency associated with the self-generated field. During one characteristic shear time $(kV)^{-1}$, the magnetic field deflects electrons by a small angle of order $\Omega_e/(kV)$. If depletion of the fundamental mode proceeds through the observed odd-harmonic hierarchy and requires three successive weak couplings, the corresponding nonlinear transfer rate scales as $\gamma_{\text{nl}} \sim kV (\Omega_e/(kV))^3$. Balancing this rate against the linear phase-mixing rate kv_{te} that populates the fundamental mode yields Eq. (8).

Further insight is provided by comparison with the 10-moment model. The fluid simulations reproduce both the linear phase-mixing growth of the fundamental mode and the emergence of odd harmonics. However, the harmonics grow algebraically in time and no saturation is observed at the amplitudes reached in the kinetic simulations. In contrast, the kinetic simulations exhibit an approximately exponential amplification of the odd harmonics on a timescale comparable to the inverse phase-mixing rate. This suggests that the odd-harmonic hierarchy results from nonlinear mode coupling, whereas the rapid transfer through that hierarchy is intrinsically kinetic and likely mediated by the phase-space structure generated by phase mixing.

Although the nonlinear saturation mechanism remains incompletely understood, Eq. (8) provides an empirical estimate for the maximum seed field generated by the slippage process. In a turbulent intracluster medium (ICM), the velocity field spans scales from an outer scale of hundreds of kpc (denoted by the subscript “out”) down to much smaller scales. To estimate the strength of the slippage seed, we assume a Kolmogorov spectrum, $V(k) \sim V_{\text{out}} (k/k_{\text{out}})^{-1/3}$, together with representative ICM parameters. For this velocity spectrum, Eq. (8) predicts $B \propto kV(k)^{2/3} \propto k^{7/9}$. Taking $L_{\text{out}} = 300$ kpc, $T_e = T_i = 10$ keV, and an outer-scale Mach number $M = V_{\text{out}}/c_s = 0.35$, this scaling implies slippage seed fields comparable to typical Biermann-battery estimates of $\sim 10^{-24}$ T at scales of order 100 pc and larger amplitudes at smaller scales. Such fields may subsequently be amplified by the turbulent dynamo, while requiring substantially less inverse magnetic energy transfer than Weibel-generated fields, which, based on the scalings of Ref. [28], are expected to emerge on scales of order μPc or smaller.

These estimates should be regarded as illustrative rather than predictive. Both the plasma conditions during the initial magnetization of the ICM and the spectrum of turbulence in initially unmagnetized collisionless plasmas remain uncertain. Nevertheless, the scaling analysis demonstrates that the slippage mechanism can produce magnetic seeds on scales far larger than kinetic plasma instabilities and with amplitudes competitive with other large-scale seed-generation mechanisms.

Pressure-anisotropy-driven microinstabilities may modify this estimate. In magnetized high- β plasmas, firehose and mirror fluctuations can scatter or trap particles, interrupt phase mixing, and reduce collisionless damping [7, 49, 50]. Similar effective collisionality in an initially weakly magnetized plasma could reduce the electron slippage that drives the present mechanism. However, these instabilities require pressure anisotropy to develop, which occurs on the same phase-mixing time that generates the lower-bound field $B_{t \sim t_{\text{pm}}}$. Thus, even in the limiting case where microinstabilities rapidly interrupt further phase mixing, fields of order $B_{t \sim t_{\text{pm}}}$ are expected. Moreover, simulations in which Weibel growth is significant still exhibit appreciable slippage-generated fields, and fully kinetic electron-ion dynamo simulations by Bacchini and Zhou (in preparation) observe the same effect. Extrapolating these results to asymptotically scale-separated astrophysical plasmas remains an open problem. The mechanism does not fundamentally require a large ion-to-electron mass ratio (in fact, it arises already in simulations with $m_i = 2m_e$), but rather different phase-mixing rates for the two species.

In conclusion, we have identified a kinetic seed-field generation mechanism that requires only spatially varying flows and arises from the phase-mixing-induced slippage of the electron flow. Unlike the Biermann battery, the mechanism operates even when both the initial magnetic field and misaligned density and temperature gra-

dients ($\nabla T \times \nabla n$) vanish identically. We derived an analytical expression for the early-time evolution of the resulting magnetic field and verified it with fully kinetic Vlasov simulations. These simulations further establish the scaling of the nonlinear saturation amplitude. While the slippage field is also present in the collisionless 10-moment model, the nonlinear saturation observed in the kinetic simulations is associated with the emergence of odd harmonics after several phase-mixing times and is not reproduced by the fluid model, suggesting that kinetic phase-space structure plays a key role in the saturation process. In the intracluster medium, the resulting seed fields can become competitive with Biermann-battery estimates while being generated on scales many orders of magnitude larger than those associated with the Weibel instability. Determining the role of this mechanism in astrophysical magnetogenesis will require future kinetic studies of weakly magnetized turbulence with greater scale separation, but the present results establish

phase-mixing-induced electron slippage as a viable source of magnetic seed fields in collisionless plasmas.

Acknowledgments: The authors are grateful for fruitful discussions with M. Zhou, F. Bacchini, P. Helander, E. Ingelsten and T. Fülöp. The work was supported by the Swedish Research Council (Dnr. 2021-03943) and the Knut and Alice Wallenberg foundation. J. Juno and the development of Gkeyll were partly funded by the NSF-CSSI program, No. 2209471. J. Juno was also supported by the U.S. Department of Energy under Contract No. DE-AC02-09CH1146 via LDRD grants. The computations were enabled by resources provided by the National Academic Infrastructure for Supercomputing in Sweden (NAISS), partially funded by the Swedish Research Council through grant agreement No. 2022-06725. The authors also acknowledge the Texas Advanced Computing Center (TACC) at The University of Texas at Austin for providing computational resources that have contributed to the research results reported within this paper.

-
- [1] R. Beck, A. Brandenburg, D. Moss, A. Shukurov, and D. Sokoloff, Galactic magnetism: Recent developments and perspectives, *Annual Review of Astronomy and Astrophysics* **34**, 155 (1996).
- [2] C. L. Carilli and G. B. Taylor, Cluster magnetic fields, *Annual Review of Astronomy and Astrophysics* **40**, 319 (2002).
- [3] K. Subramanian, The origin, evolution and signatures of primordial magnetic fields, *Reports on Progress in Physics* **79**, 076901 (2016).
- [4] F. Govoni and L. Feretti, Magnetic fields in clusters of galaxies, *International Journal of Modern Physics D* **13**, 1549 (2004), <https://doi.org/10.1142/S0218271804005080>.
- [5] R. M. Kulsrud and E. G. Zweibel, On the origin of cosmic magnetic fields, *Reports on Progress in Physics* **71**, 046901 (2008).
- [6] A. Brandenburg and E. Ntormousi, Galactic dynamos, *Annual Review of Astronomy and Astrophysics* **61**, 561 (2023).
- [7] M. W. Kunz, A. A. Schekochihin, and J. M. Stone, Firehose and mirror instabilities in a collisionless shearing plasma, *Phys. Rev. Lett.* **112**, 205003 (2014).
- [8] I. Zhuravleva, E. Churazov, A. A. Schekochihin, S. W. Allen, A. Vikhlinin, and N. Werner, Suppressed effective viscosity in the bulk intergalactic plasma, *Nature Astronomy* **3**, 832 (2019).
- [9] S. V. Komarov, E. M. Churazov, M. W. Kunz, and A. A. Schekochihin, Thermal conduction in a mirror-unstable plasma, *Monthly Notices of the Royal Astronomical Society* **460**, 467 (2016).
- [10] G. T. Roberg-Clark, J. F. Drake, C. S. Reynolds, and M. Swisdak, Suppression of electron thermal conduction in the high β intracluster medium of galaxy clusters, *The Astrophysical Journal Letters* **830**, L9 (2016).
- [11] G. T. Roberg-Clark, J. F. Drake, C. S. Reynolds, and M. Swisdak, Suppression of electron thermal conduction by whistler turbulence in a sustained thermal gradient, *Phys. Rev. Lett.* **120**, 035101 (2018).
- [12] J. H. Matthews, A. R. Bell, and K. M. Blundell, Particle acceleration in astrophysical jets, *New Astronomy Reviews* **89**, 101543 (2020).
- [13] T. Amano, Y. Matsumoto, A. Bohdan, O. Kobzar, S. Matsukiyo, M. Oka, J. Niemiec, M. Pohl, and M. Hoshino, Nonthermal electron acceleration at collisionless quasi-perpendicular shocks, *Reviews of Modern Plasma Physics* **6**, 29 (2022).
- [14] F. Guo, Y.-H. Liu, S. Zenitani, and M. Hoshino, Magnetic reconnection and associated particle acceleration in high-energy astrophysics, *Space Science Reviews* **220**, 43 (2024).
- [15] L. Sironi, D. A. Uzdensky, and D. Giannios, Relativistic magnetic reconnection in astrophysical plasmas: A powerful mechanism of nonthermal emission, *Annual Review of Astronomy and Astrophysics* **63**, 127 (2025).
- [16] M. R. Krumholz and C. Federrath, The role of magnetic fields in setting the star formation rate and the initial mass function, *Frontiers in Astronomy and Space Sciences* **6**, 7 (2019).
- [17] P. F. Hopkins, But what about...: Cosmic rays, magnetic fields, conduction and viscosity in galaxy formation, *Monthly Notices of the Royal Astronomical Society* **492**, 3465 (2020).
- [18] A. Bonafede, L. Feretti, M. Murgia, F. Govoni, G. Giovannini, D. Dallacasa, K. Dolag, and G. B. Taylor, The Coma cluster magnetic field from Faraday rotation measures, *Astronomy and Astrophysics* **513**, A30 (2010).
- [19] L. Feretti, G. Giovannini, F. Govoni, and M. Murgia, Clusters of galaxies: Observational properties of the diffuse radio emission, *The Astronomy and Astrophysics Review* **20**, 54 (2012).
- [20] R. M. Crutcher, Magnetic fields in molecular clouds, *Annual Review of Astronomy and Astrophysics* **50**, 29 (2012).
- [21] A. Brandenburg and K. Subramanian, Astrophysical magnetic fields and nonlinear dynamo theory, *Physics*

- Reports **417**, 1 (2005).
- [22] F. Rincon, Dynamo theories, *Journal of Plasma Physics* **85**, 205850401 (2019).
- [23] L. Biermann, Über den ursprung der magnetfelder auf sternern und im interstellaren raum, *Zeitschrift für Naturforschung A* **5**, 65 (1950).
- [24] J.-B. Durive and M. Langer, Intergalactic magnetogenesis at cosmic dawn by photoionization, *Monthly Notices of the Royal Astronomical Society* **453**, 345 (2015), <https://academic.oup.com/mnras/article-pdf/453/1/345/4913470/stv1578.pdf>.
- [25] M. Langer and J.-B. Durive, Magnetizing the cosmic web during reionization, *Galaxies* **6**, 124 (2018).
- [26] E. S. Weibel, Spontaneously growing transverse waves in a plasma due to an anisotropic velocity distribution, *Phys. Rev. Lett.* **2**, 83 (1959).
- [27] M. Zhou, V. Zhdankin, M. W. Kunz, N. F. Loureiro, and D. A. Uzdensky, Spontaneous magnetization of collisionless plasma, *Proceedings of the National Academy of Sciences* **119**, e2119831119 (2022), <https://www.pnas.org/doi/pdf/10.1073/pnas.2119831119>.
- [28] M. Zhou, V. Zhdankin, M. W. Kunz, N. F. Loureiro, and D. A. Uzdensky, Magnetogenesis in a collisionless plasma: From Weibel instability to turbulent dynamo, *The Astrophysical Journal* **960**, 12 (2023).
- [29] F. Pucci, M. Viviani, F. Valentini, G. Lapenta, W. H. Matthaeus, and S. Servidio, Turbulent magnetogenesis in a collisionless plasma, *The Astrophysical Journal Letters* **922**, L18 (2021).
- [30] L. Sironi, L. Comisso, and R. Golant, Generation of near-equipartition magnetic fields in turbulent collisionless plasmas, *Phys. Rev. Lett.* **131**, 055201 (2023).
- [31] M. V. Medvedev and A. Loeb, Generation of magnetic fields in the relativistic shock of gamma-ray burst sources, *The Astrophysical Journal* **526**, 697 (1999).
- [32] Z. Liu, M. Zhou, and N. F. Loureiro, Suppression of inverse magnetic energy transfer in collisionless marginally magnetized plasmas, *The Astrophysical Journal Letters* **995**, L46 (2025).
- [33] F. Rincon, F. Califano, A. A. Schekochihin, and F. Valentini, Turbulent dynamo in a collisionless plasma, *Proceedings of the National Academy of Sciences* **113**, 3950 (2016), <https://www.pnas.org/doi/pdf/10.1073/pnas.1525194113>.
- [34] D. A. St-Onge and M. W. Kunz, Fluctuation dynamo in a collisionless, weakly magnetized plasma, *The Astrophysical Journal Letters* **863**, L25 (2018).
- [35] I. Pusztai, J. Juno, A. Brandenburg, J. M. TenBarge, A. Hakim, M. Francisquez, and A. Sundström, Dynamo in weakly collisional nonmagnetized plasmas impeded by Landau damping of magnetic fields, *Phys. Rev. Lett.* **124**, 255102 (2020).
- [36] L. Hanebring, J. Juno, A. Hakim, J. TenBarge, and I. Pusztai, From weibel seeds to dynamo beyond pair-plasmas, *Journal of Plasma Physics* **92**, E79 (2026).
- [37] G. Schubert and K. Soderlund, Planetary magnetic fields: Observations and models, *Physics of the Earth and Planetary Interiors* **187**, 92 (2011), special Issue: Planetary Magnetism, Dynamo and Dynamics.
- [38] S. M. Tobias, The turbulent dynamo, *Journal of Fluid Mechanics* **912**, P1 (2021).
- [39] P. J. Käpylä, M. K. Browning, A. S. Brun, G. Guerrero, and J. Warnecke, Simulations of solar and stellar dynamos and their theoretical interpretation, *Space Science Reviews* **219**, 58 (2023).
- [40] A. A. Schekochihin, S. C. Cowley, S. F. Taylor, J. L. Maron, and J. C. McWilliams, Simulations of the small-scale turbulent dynamo, *The Astrophysical Journal* **612**, 276 (2004).
- [41] D. H. Porter, T. W. Jones, and D. Ryu, Vorticity, shocks, and magnetic fields in subsonic, ICM-like turbulence, *The Astrophysical Journal* **810**, 93 (2015).
- [42] F. Vazza, G. Brunetti, M. Brüggén, and A. Bonafede, Resolved magnetic dynamo action in the simulated intracluster medium, *Monthly Notices of the Royal Astronomical Society* **474**, 1672 (2017), <https://academic.oup.com/mnras/article-pdf/474/2/1672/22473785/stx2830.pdf>.
- [43] M. J. Korpi-Lagg, M.-M. Mac Low, and F. A. Gent, Computational approaches to modeling dynamos in galaxies, *Living Reviews in Computational Astrophysics* **10**, 3 (2024).
- [44] A. B. Mikhailovskii, Oscillations of an isotropic relativistic plasma, *Plasma Physics* **22**, 133 (1980).
- [45] J. Juno, A. Hakim, J. TenBarge, E. Shi, and W. Dorland, Discontinuous galerkin algorithms for fully kinetic plasmas, *Journal of Computational Physics* **353**, 110 (2018).
- [46] Gkeyll page on GitHub, <https://github.com/ammarrhakim/gkeyll>, Accessed: 2026-05-20.
- [47] L. Wang, A. H. Hakim, A. Bhattacharjee, and K. Germaschewski, Comparison of multi-fluid moment models with particle-in-cell simulations of collisionless magnetic reconnection, *Physics of Plasmas* **22**, 012108 (2015).
- [48] L. Wang, A. H. Hakim, J. Ng, C. Dong, and K. Germaschewski, Exact and locally implicit source term solvers for multifluid-Maxwell systems, *Journal of Computational Physics* **415**, 109510 (2020).
- [49] M. W. Kunz, J. Squire, A. A. Schekochihin, and E. Quataert, Self-sustaining sound in collisionless, high-beta plasma, *Journal of Plasma Physics* **86**, 905860603 (2020).
- [50] R. Meyrand, A. Kanekar, W. Dorland, and A. A. Schekochihin, Fluidization of collisionless plasma turbulence, *Proceedings of the National Academy of Sciences* **116**, 1185 (2019).